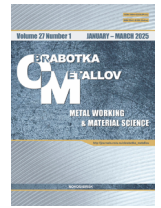# Obrabotka metallov -
Metal Working and Material Science

Journal homepage: http://journals.nstu.ru/obrabotka_metallov

Influence of the oscillating systems inclination angle on the surface properties of steel 45 during ultrasonic surface plastic deformation

Dmitry Fatyukhin [a], Ravil Nigmetzyanov [b], Vyacheslav Prikhodko [c], Sergey Sundukov [d], Aleksandr Sukhov [e]

Moscow Automobile and Road Construction State Technical University (MADI), 64 Leningradsky prospect, Moscow, 125319, Russian Federation

[a] https://orcid.org/0000-0002-5914-3415, ✉ mitriy2@yandex.ru; [b] https://orcid.org/0009-0008-1443-7584, ✉ lefmo@yandex.ru;
[c] https://orcid.org/0000-0001-8261-0424, ✉ prikhodko@madi.ru; [d] https://orcid.org/0000-0003-4393-4471, ✉ sergey-lefmo@yandex.ru;
[e] https://orcid.org/0009-0009-9097-8216, ✉ sukhov-aleksandr96@mail.ru

ARTICLE INFO

ABSTRACT

Introduction. Among the methods of modifying the surfaces of metal products to change the physical-mechanical and geometric properties of the surface layer, surface plastic deformation (*SPD*) methods are the most prevalent. Using ultrasound to enhance the efficiency of deformation processes allows for increase in microhardness and reduction in roughness compared to rolling and smoothing. The greatest technological challenges are caused by ultrasonic surface plastic deformation of curved surfaces, including those obtained by additive technologies. Given that most ultrasonic *SPD* methods are based on the longitudinal nature of vibrations, to ensure uniform processing of curved surfaces, the tool axis should be oriented at a specific angle relative to any point on the surface being processed. In this regard, **the purpose of the work** is to study the effect of the oscillating system inclination angle on the surface properties of steel 45 during ultrasonic surface plastic deformation. This study examines steel 45 samples subjected to ultrasonic *SPD* at various oscillating system inclination angles: 90°, 75°, 60°, and 45°. **Methods.** The research methods included metallographic studies of the surface layer microstructure of the samples, measurement of its microhardness and roughness, as well as comparative wear tests. **Results and discussion.** Ultrasonic surface deformation, at any of the considered tool inclination angles α, creates a hardened layer – from 30 μm at $\alpha = 45°$ to 350 μm at $\alpha = 90°$. In this case, the microhardness increases to 240 HV at $\alpha = 45°$. Furthermore, at any α, there is a significant decrease in roughness. For example, altitude parameters are reduced by more than 8 times. The best results were achieved at $\alpha = 60°$. The wear test results indicated a substantial reduction in weight loss due to wear following ultrasonic processing. The most significant decrease in wear (more than twofold) was observed at an inclination angle of $\alpha = 90°$.

Introduction

Reliability requirements for modern equipment are based on the operational performance of parts and assembly units, such as wear resistance, fatigue strength, corrosion resistance, etc. These properties are largely determined by the complex of physical, mechanical, and geometric characteristics of the surface layers of the parts. Currently, a wide range of technological methods exists for forming the structure, microhardness, and roughness and sub-roughness parameters. Methods that provide the desired surface characteristics without material removal are particularly in demand. These primarily include surface plastic deformation (*SPD*) methods [1].

* **Corresponding author**
Fatyukhin Dmitriy S., D.Sc. (Engineering), Associate Professor
Moscow Automobile and Road Construction
State Technical University (MADI),
64 Leningradsky prospect,
125319, Moscow, Russian Federation
Tel.: +7 968 868-60-73, **e-mail:** mitriy2@yandex.ru

Both static and dynamic *SPD* methods can be significantly improved by applying ultrasonic vibrations to the working tool [2]. This technological approach allows for a substantial increase in the degree of strain hardening and hardness, as well as a reduction in roughness and the creation of a regular microrelief.

The intensification of *SPD* processes using ultrasound is widely applied. A significant body of work, both fundamental [4, 8, 9] and applied [14, 15, 16], is dedicated to this type of processing.

Two primary schemes for ultrasonic *SPD* are based on the use of deforming elements that are either rigidly connected to the oscillating system or are not rigidly connected to the vibration source [23].

In 1964, I.I. Mukhanov first proposed a method of ultrasonic *SPD* using a working tool rigidly connected to the oscillating system [21]. Further developing this method, I.A. Stebelkov patented a type of processing using free working bodies in 1975 [22]. A rigidly connected working tool allows for more uniform processing and results in lower surface roughness than processing with a free deforming element [3, 6]. However, processing with a free deforming element can achieve a greater degree of strain hardening and a deeper hardened layer [25].

One of the main areas of research in ultrasonic *SPD* is the study of the influence of this processing method on the structure and properties of various materials based on iron [5, 7], titanium, aluminum, etc. [11–13]. Recently, this trend has been devolving in the field of nanotechnology [20, 26].

Most technical solutions for ultrasonic *SPD* are based on transmitting longitudinal vibrations to the working tool. Ultrasonic smoothing, used to achieve the lowest possible roughness, can be implemented according to three processing schemes, as shown in Fig. 1.
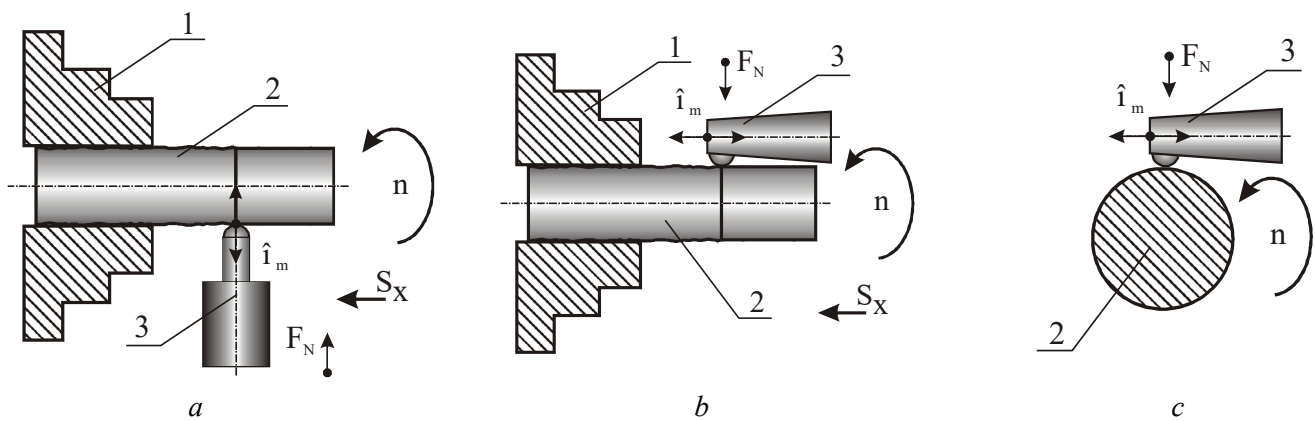

Fig. 1. Surface plastic deformation (*SPD*) processing schemes:
a – with normal vibrations; *b, c* with tangential vibrations (1 – chuck, 2 – workpiece, 3 – tool)

The processing of curved surfaces, including those produced by additive manufacturing technologies, presents the greatest challenges [33–36].

When the oscillating system with the tool moves rectilinearly along a curved surface, their force interaction can vary significantly. The tool axis deviates from the normal to the surface, and the static pressing force F is decomposed into components (Fig. 2).

When the tool axis is positioned at an angle of $\alpha = 90°$ and the static pressing force is F, there is only a normal component of this force F_N, i.e., $F = F_N$. When $\alpha \neq 90°$, in addition to the normal component F_N, a tangential component F_τ also appears. In this case, $F_N = F \cdot \sin\alpha$, and $F_\tau = F \cdot \cos\alpha$. The periodic force generated by the tool changes in the same way.

The nature of the impact on the surface also changes accordingly. At $\alpha = 90°$ and $F_N = F_{Nmax}$, each vibration of the tool leaves a spherical imprint on the surface, with the maximum normal strain occurring at the center of the imprint (Fig. 3, *a*). At $\alpha \neq 90°$ and with the presence of the component F_τ, the tool slides along the surface, and the imprints are elongated. Normal strains dominate at the beginning of the imprint, while shear strains dominate at the end (Fig. 3, *b*). That is, by analogy with static methods of *SPD*, at $\alpha = 90°$ the process is carried out according to a smoothing scheme, while at $\alpha \neq 90°$ it is carried out according to a vibrational smoothing scheme.
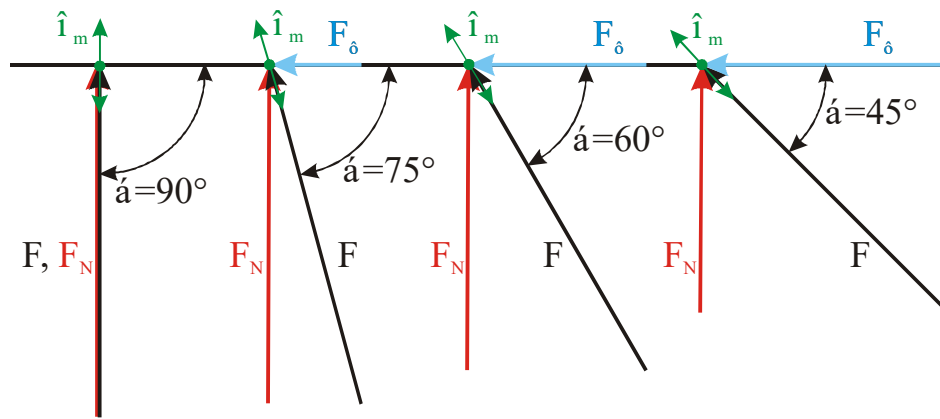
Fig. 2. Change in the normal F_N and tangential F_τ components of the interaction force between the tool and the workpiece surface at different tool inclination angles α (ξ_m – the amplitude of vibrations of the ultrasonic emitter)

Considering the longitudinal nature of the vibrations, to ensure uniform processing of curved surfaces, the tool axis must be directed at a specified angle to any section of the surface being processed.

In order to improve the processing quality of surfaces with complex geometries, ultrasonic *SPD* methods are being improved and modernized [17, 19]. Methods using multi-element deforming tools [23, 24] have emerged, as well as hybrid methods combining features of smoothing and impact processing [27, 28] or a combination of *SPD* with thermal [31, 32] and thermochemical processing [29, 30].

In this regard, ***the aim of this work*** is to study the influence of the oscillation system's inclination angle on the surface properties of steel 45 under ultrasonic *SPD*. To achieve this aim, ***the following tasks were addressed***:

● to analyze the change in microstructure of the specimens processed by ultrasonic *SPD*;

● to evaluate the changes in microhardness and roughness of the specimens;

● to conduct comparative wear tests on the specimens;

● to propose technological recommendations for the effective application of ultrasonic *SPD* at various oscillation system's inclination angles.

Fig. 3. Traces (**1**) and cross-sections of traces (**2**) of the working tool traces on the sample surface: *a* – at $\alpha = 90°$; *b* – at $\alpha \neq 90°$

Research procedure

Materials and methods for specimen preparation

A hot-rolled bar made of 45 mm structural steel with a diameter of 42 mm was used for experimental studies. Cylindrical specimens, 300 mm in length, were machined from the bar. The chemical composition of the steel was determined by spectral analysis using a *Foundry-Master LAB* spectrometer (SYNERCON LLC, Moscow, Russia). The composition is shown in Table.

Chemical composition of steel 45 (%)

Material	C	Cr	Mn	Ni	Cu	W	Si	Fe
Steel 45	0.46	0.09	0.55	0.27	0.1	0.01	0.21	98.31

The specimens were machined on a single precision lathe *16E20* (Alma Ata Machine Tool Plant, Alma Ata, Kazakhstan). A surface layer of 0.75 mm thickness was removed from the specimens, followed by contour turning with the following parameters: feed rate $S_X = 0.34$ mm/rpm, spindle rotation speed $n = 560$ rpm, and cutting depth $t = 0.25$ mm. The contour turning, using a tool with a tip radius of 0.4 mm, resulted in a regular microrelief of the surface with the surface roughness parameters: $R_a = 6.63$ μm, $R_z = 30.1$ μm, $R_{max} = 33.7$ μm, $S_m = 0.260$ mm, $S = 0.055$ mm, $t_{30} = 11.6\%$. These values are consistent with rough machining. The selection of specimen processing mode was based on an analysis of previous studies, for example, [37].

Grooves with a depth of 3–4 mm were made on the specimens every 50 mm, to divide the specimen surface into sections.

Similar specimens, made according to the above procedure, were used to study the effect of the tilt angle of the oscillating system on the change in the properties of steel 45 under the influence of ultrasonic *SPD*.

After machining, the specimens were normolized at $T = 860$ °C. The microhardness on the surface of the specimens was 165 HV 20, and the core material, it was 125 HV 20.

Experimental procedure and equipment

Ultrasonic *SPD* was performed according to the scheme shown in Fig. 4. An ultrasonic oscillating system with a waveguide concentrator was mounted in the tool holder of the lathe. A rod-type, three-half-wavelength magnetostrictive oscillating system *PMS-2.0/22* (Afalina LLC, Moscow, Russia) was used. It consists of a magnetostrictive transducer made of *49K2F* alloy, located in a water-cooling casing, and a waveguide concentrator made of titanium alloy soldered to its end.

To ensure the indenter is pressed against the workpiece surface with the necessary force, the oscillating system is equipped with a spring that provides a defined clamping force. A stepped titanium emitter with a transmitting surface diameter of Ø16 mm, which has a vibration amplitude amplification factor of $k_y = 2$, was connected to the waveguide of the oscillating system via a threaded connection. A *WC8* hard
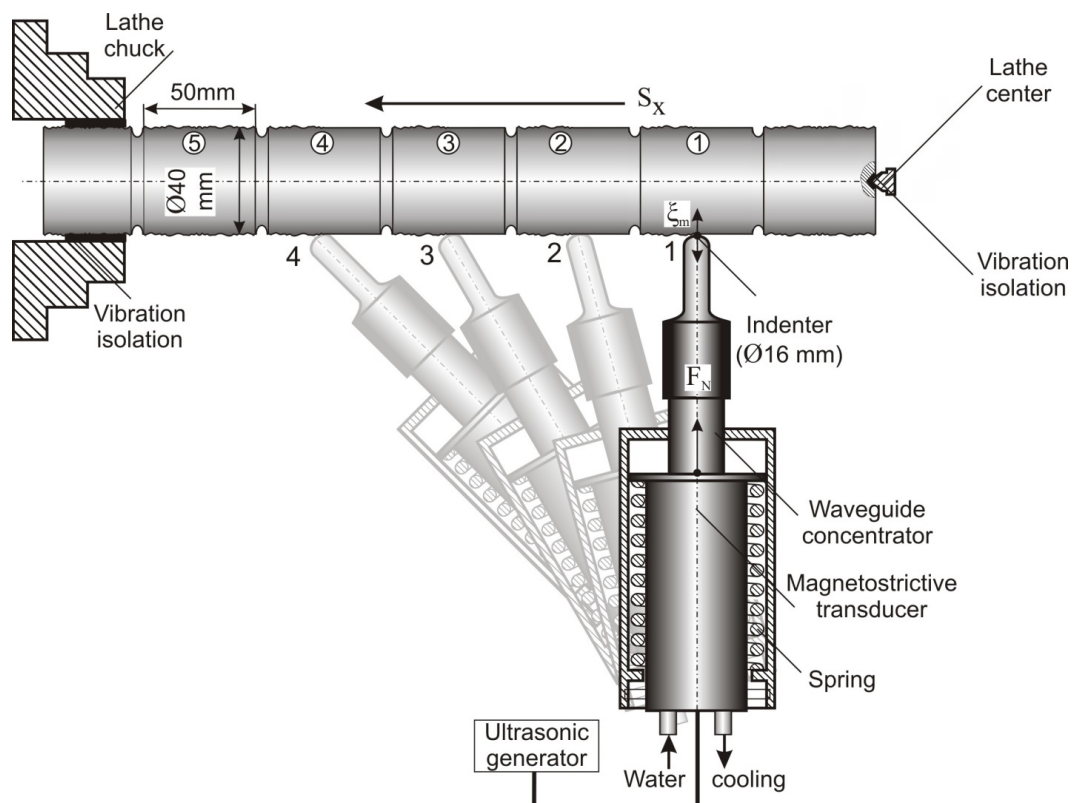

Fig. 4. Design of an experiment

alloy indenter was soldered to the working end of the emitter. The indenter is a 6 mm thick plate in the shape of a circle segment with a diameter of 16 mm. The edge of the plate is rounded.

The oscillating system was powered by a generator *UZG2-22* (Afalina LLC, Moscow, Russia) with a maximum output power of 2 kW. The generator has automatic frequency control (*AFC*) and amplitude control functions, which allows changing the resonant frequency when the mechanical load at the end of the emitter changes.

An electrodynamic vibrometer was used to measure the amplitude of oscillatory displacements ξ_m. This consists of a magnetic system comprising an annular permanent magnet (*TU 48-1301-16–73*), a measuring coil on a plexiglass frame containing 800 turns of *PEV2-0.1* wire, and disc-shaped magnetic cores. The vibrometer was positioned on a waveguide of a rod oscillating system.

To evaluate the maximum vibration amplitude ξ_m, the vibrometer was calibrated optically using a microscope. During operation of the oscillating system, the signal from the electrodynamic vibrometer was fed to a voltmeter, the scale of which was calibrated using the microscope.

The specimen was secured in the lathe chuck on one end and supported by the lathe center on the other. To prevent the transmission of high-frequency vibrations to the chuck and center, they were equipped with *PTFE* (Teflon) vibration isolation pads.

The lathe spindle speed was set to n = 560 rpm, which provides a processing speed of approximately $V_r \approx 1.2$ m/s for the chosen specimen. Literature analysis [25, 26] and preliminary experiments indicate that changes in spindle speed have a negligible effect on changes in hardness and roughness. When varying the speed over a wide range, the roughness, with all other parameters held constant, changed by no more than 8–12 %, and the change in hardness did not exceed 10 %. Moreover, increasing the speed significantly increases the indenter temperature.

Based on an analysis of *SPD* studies and preliminary experimental data, the following ultrasonic processing parameters were selected: longitudinal feed S_X, oscillation amplitude ξ_{max} and clamping force F_N.

For the given material and processing conditions, decreasing the feed rate *Sx* of the tool increases the technological effect, but significantly reduces the processing productivity. Therefore, a value of S_X = 0.24 mm/rev was selected. The vibration amplitude was selected within the range of ξ_{max} = 8–10 μm, since the most significant reduction in surface roughness is observed at these amplitudes. Increasing the clamping force above F_N = 100–120 N does not lead to a significant result, so processing was performed at F_N = 100 N.

The study of the influence of the oscillating systems' inclination angle on the properties of the deformed layer was carried out as follows:

When processing the specimen according to the scheme shown in Fig. 4, the oscillating system with the working tool (indenter) was installed in the tool holder at an angle of α = 90° to the specimen surface in section **1**. After processing section **1**, the position of the oscillating system was changed by rotating the tool holder. During processing of section **2**, the inclination angle α of the oscillating system was 75°; during processing of section **3** it was 60°, and during processing of section **4** it was 45°. Section **5** was retained as a control specimen.

An example of processing the specimen sections at the oscillating systems' inclination angles of 75° and 45° is shown in Fig. 5.

Assessment of surface microgeometry

The standard surface roughness parameters according to *GOST 2789–73* were assessed on the control and processed samples: arithmetic mean deviation of the profile R_a, height of irregularities over 10 points R_z, maximum height of the profile irregularities R_{max}, mean spacing of profile irregularities S_m, mean spacing of local peaks S, and relative bearing length of the profile t_p, where p is the level of the profile section. The level of the profile section p was taken to be 30 % during measurements.

The surface roughness parameters were measured on a profilometer *Model 130* (Proton JSC, Zelenograd, Russia).
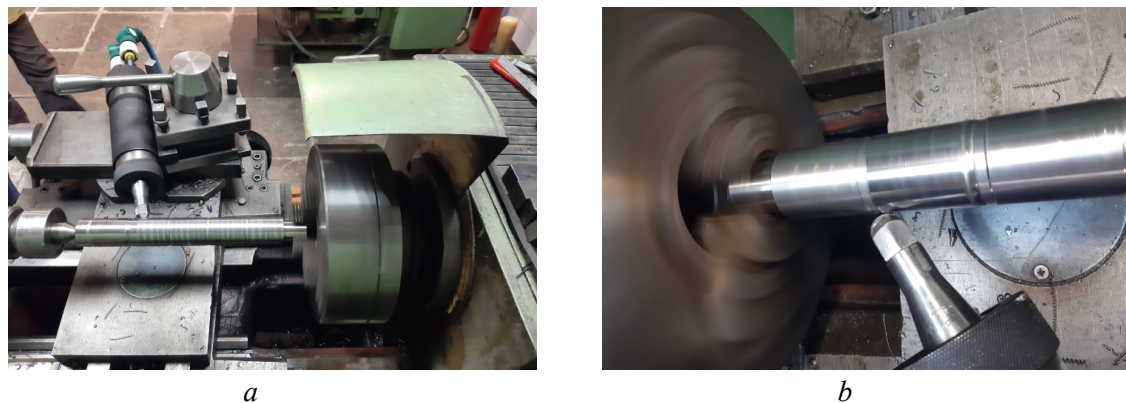
Fig. 5. Processing of sample sections at oscillating system inclination angles of:
a – 75° and *b* – 45°

When plotting the dependencies of the roughness parameters, the values were taken as the arithmetic mean of five measurements at different sections of the specimen. The obtained experimental data were approximated using the least squares method. Numerical and graphical processing of the measurement results was performed in the *Statistica* program. Since the spread of the obtained values did not exceed the 3σ interval, the data can be considered reliable.

Assessment of the surface structure and properties

The microstructure and microhardness of the control and processed specimens were also assessed.

The microstructure was studied using a metallographic microscope *METAM RV-22* (LOMO JSC, St. Petersburg, Russia), which is an inverted microscope with a top stage. The microscope is designed for visual observation of the microstructure of metals, alloys, and other opaque objects in reflected light under direct illumination in brightfield and darkfield modes. The magnification range is 80×–1,000×.

The microhardness of the specimens was measured using a *PMT-3* microhardness tester (LOMO JSC, St. Petersburg, Russia) according to the procedure based on *GOST 2999–75*. The depth of the modified layer was determined in a normal section.

Assessment of friction and wear

The obtained samples were subjected to friction and wear tests. The tests were performed using a universal friction machine *MTU-01* (Prodvinutie Tekhnologii LLC, Moscow) [38] according to *TU 32.99.53-001-78940767–2018*.

The tests were conducted without the use of lubricants on specimens representing a segment of the cylinder specimen. A cup made of steel 45 with an outer diameter of 34 mm and a wall thickness of 10 mm was used as the counterbody.

The friction torque and axial load on the machine spindle were recorded using *MTU-01* strain gauges.

The contact scheme: the end of the rotating cup and the cylindrical surface of the specimen. Graphical representation of the changes in the registered parameters is recorded and processed by a computer using the software module *QMbox*.

Wear during friction was determined by the change in weight of the tested specimens before and after the testing using analytical balance *GF-1000* (A&D Company, Limited, Japan) with a sampling rate of 0.001 g.

Results and Discussion

Roughness

The results presented in Fig. 6 were obtained under the selected ultrasonic surface deformation mode.

In the presented graphs, the roughness values at $\alpha = 0°$ were obtained on specimens after turning with the selected mode but without ultrasonic exposure. The remaining dependencies were obtained during processing the specimens with tool inclination angles in the range of 45°–90°. A significant reduction in
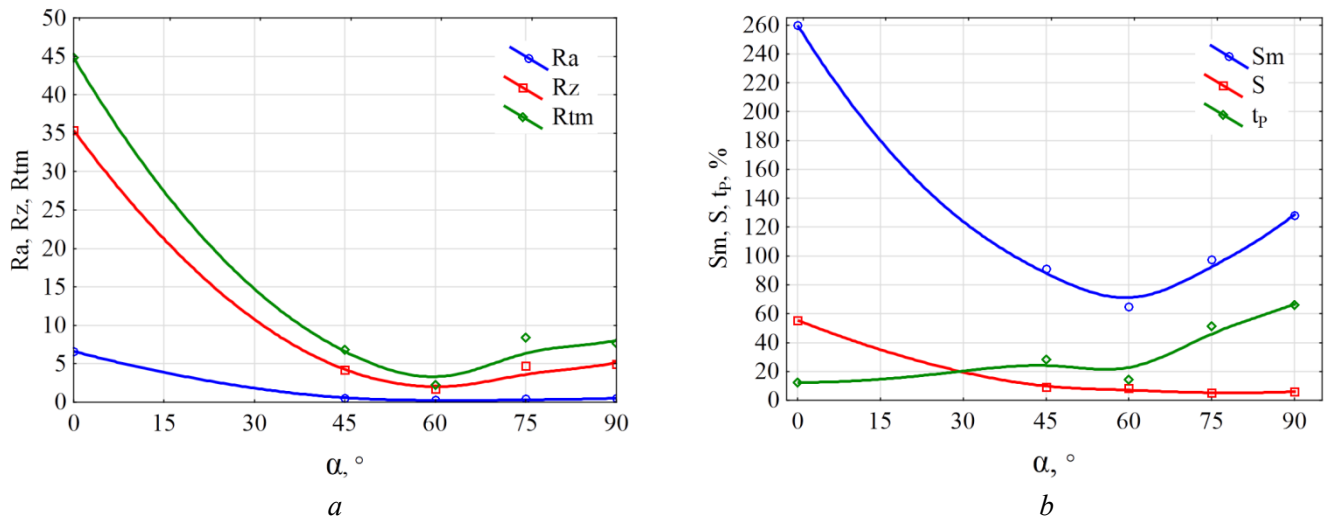
Fig. 6. Dependence of the change in the roughness parameters on the tool inclination angle **α**:

a – altitude R_a, R_z, R_{tm} and *b* – spacing S_m, S, t_p

height and spacing parameters of roughness, as well as an increase in t_p, is observed for all specimens. The smallest changes are observed with a tool inclination angle of **α = 90°**, and the largest changes occur at **α = 60°**. This pattern of changes is related to the fact that as **α** decreases, the tangential component of the static clamping force F_τ increases, and, consequently, shear strains increase.

Fig. 7 shows the surface profilograms of the specimens before and after ultrasonic processing with different inclination angles of the working tool.

R_{max} = 45 μm

a

R_{max} = 7.6 μm

b

R_{max} = 8.4 μm

c

R_{max} = 2.4 μm

d

R_{max} = 7.4 μm

e
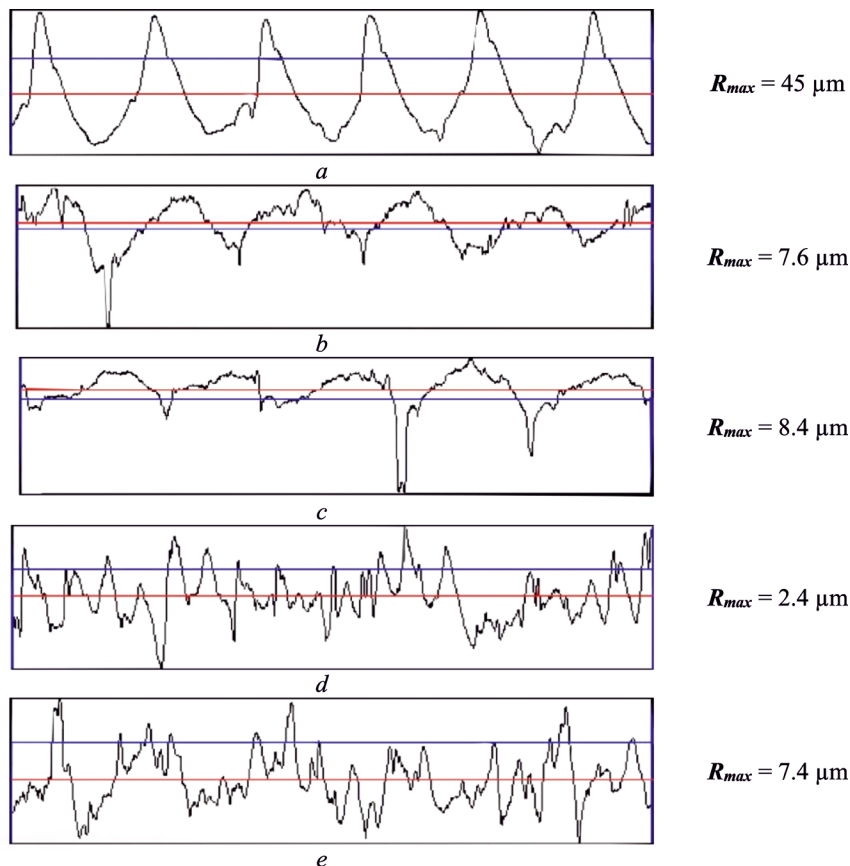
Fig. 7. Surface profiles obtained at different working tool inclination angles:

a – without *SPD*; *b* – at **α = 90°**; *c* – at **α = 75°**; *d* – at **α = 60°**; *e* – at **α = 45°**

The formation of a regular microrelief is clearly visible in the profilograms when processing with tool inclination angles of 90° and 75°. At smaller angles, the regularity is disrupted, but a greater change in roughness parameters occurs.

Structure, hardness and microhardness

When a significant clamping force is applied, the deforming element and emitter oscillate in common mode, i.e., the tool does not detach from the workpiece surface, and the processing conditions are close to smoothing. The main mechanism creating deformation of the surface layer is loading the workpiece surface with a ball under the action of a static clamping force and a significantly larger dynamic force created by the emitter vibrations. This results in both hardening and smoothing of the surface.

Obviously, when the tool inclination angle is $\alpha = 90°$, the force acting on the surface has only one normal component, F_N, which creates the most favorable conditions for surface hardening (work hardening). As the angle decreases, the normal component F_N decreases, and the tangential component F_τ increases. This leads to a decrease in hardness and a reduction in the depth of the hardened layer, but it also reduces the size of micro-irregularities due to smoothing.

The results of metallographic studies are presented in Fig. 8.

As the experimental results show (Fig. 9), the depth of the work-hardened layer increases with an increase in the inclination angle α of the working tool. At $\alpha = 45°$, changes in the structure and properties extend to a depth of up to 50 μm, and at $\alpha = 90°$, the depth reaches 345 μm.

Obviously, the depth of the deformed layer is determined by the magnitude of the normal component F_N of the force. At the same time, the highest microhardness at a depth of up to 50 μm is achieved at $\alpha = 45°$, which is related to the shear strains created by the tangential component F_τ.

Friction torque and wear

Comparative wear tests of the specimens were carried out at a constant clamping force between the specimen and the counterbody $N = 25$ N. The spindle speed was $n = 160$ rpm. As a result, the dependence of the change in friction torque M_{fr} over 1,000 cycles was obtained (Fig. 10).
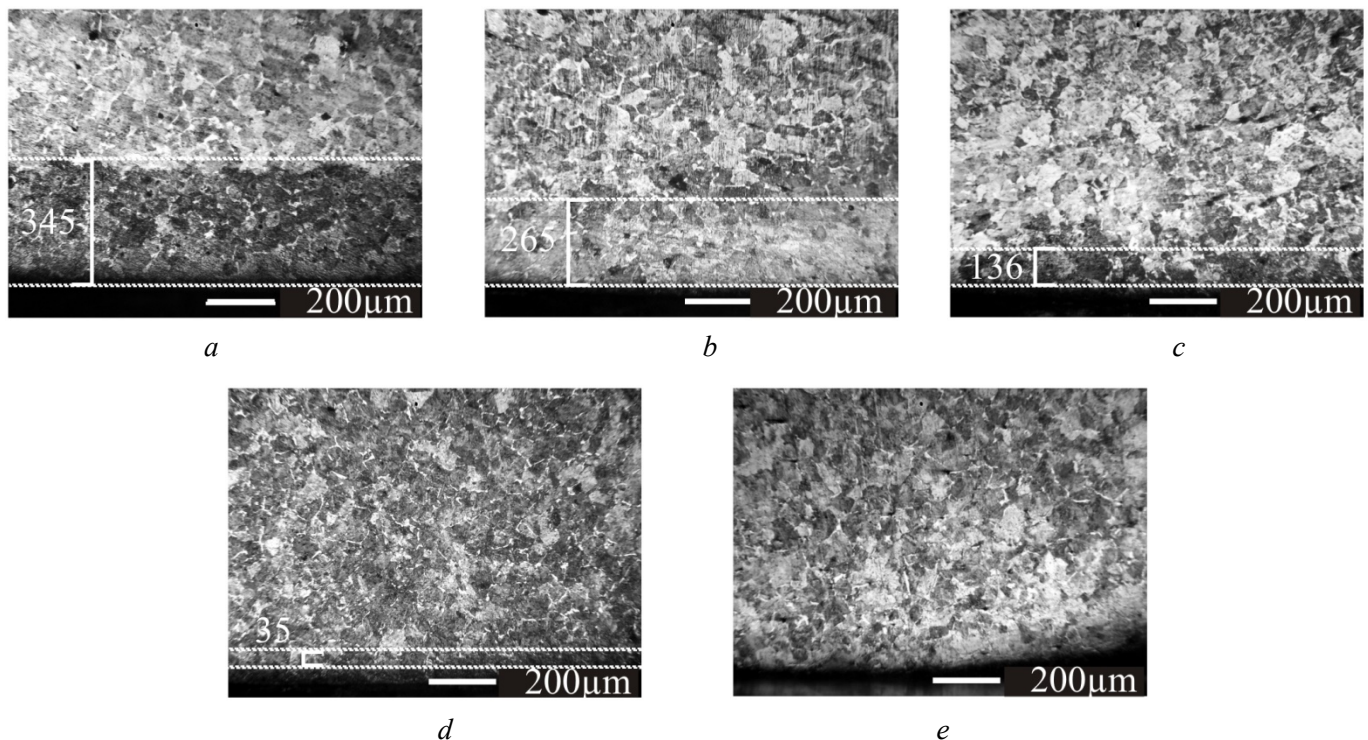

Fig. 8. Microstructures of samples obtained at different working tool inclination angles:

a – at $\alpha = 90°$; *b* – at $\alpha = 75°$; *c* – at $\alpha = 60°$; *d* – at $\alpha = 45$; *e* – without *SPD*
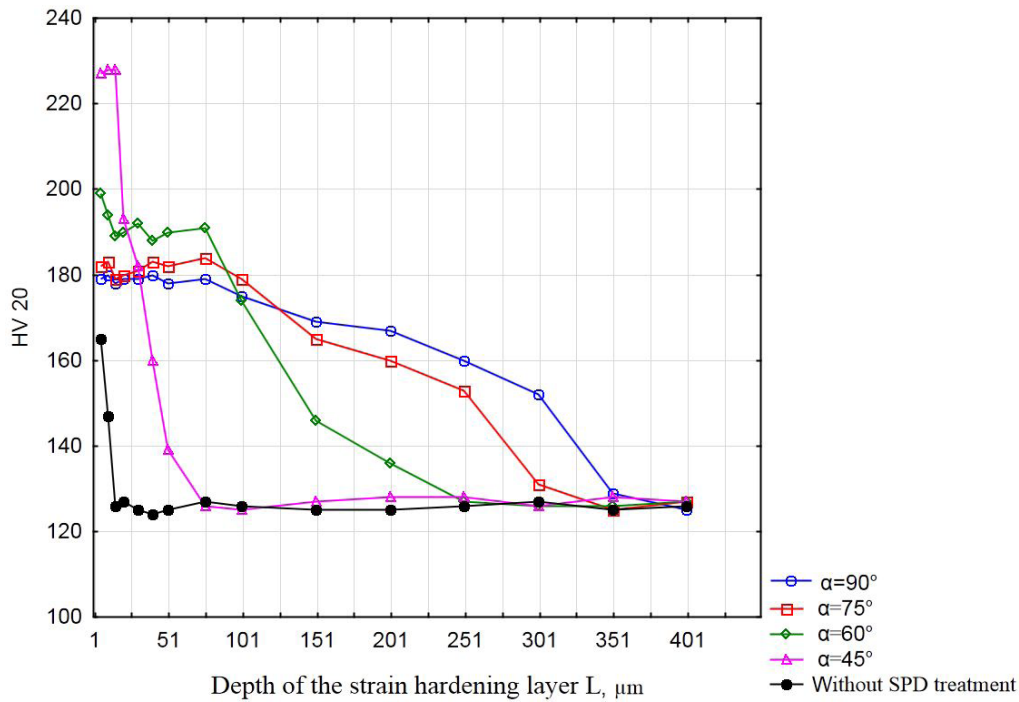
Fig. 9. Hardened layer depth **L** at different working tool inclination angles **α**
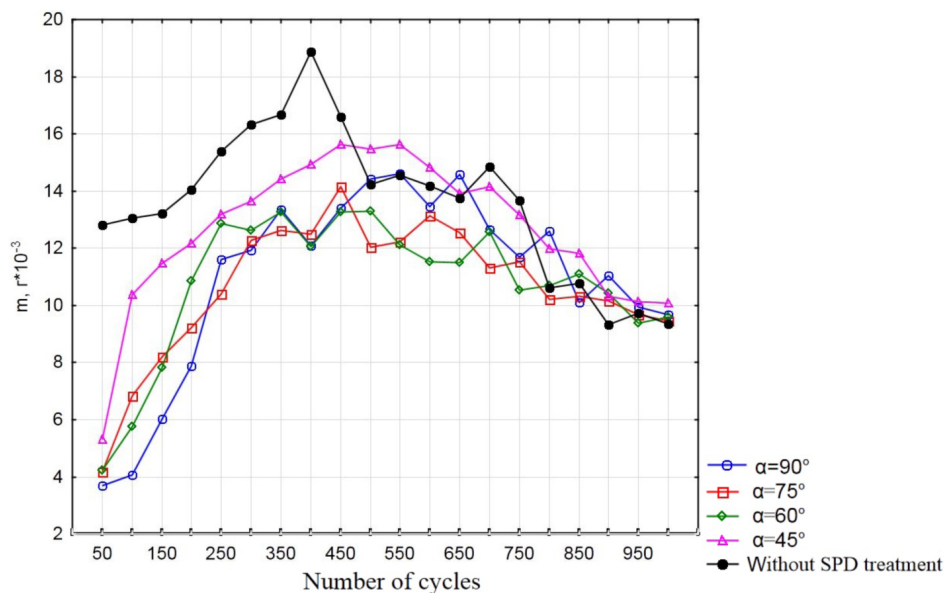

Fig. 10. Wear dynamics of samples obtained at different working tool
inclination angles **α**

Both the increase in hardness and the decrease in roughness have a certain effect on the friction and wear processes. The results of the conducted studies show that the friction torque M_{fr} for all tested specimens increases over 450–550 cycles.

The highest friction torques are observed during the wear of the surface layer, which corresponds to the running-in period for specific friction conditions. When an equilibrium roughness is formed on the specimens, the friction torque M_{fr} begins to decrease.

The highest friction torque M_{fr} was observed in the specimen without *SPD* processing. In the specimens processed with *SPD* at various inclination angles **α** of the working tool, a significantly lower M_{fr} was recorded, indicating a reduction in wear. After reaching the wear depth in the specimens corresponding to the depth of the deformed layer, the process stabilizes, and for a duration of 850–1,000 cycles, the dynamics of the change in friction torque M_{fr} become similar for all specimens.

Before and after the friction tests, the specimens were weighed. As the inclination angle of the oscillating system decreased, the amount of wear by mass increased. The lowest wear (0.146 g) was recorded in the specimens processed at an inclination angle of $\alpha = 90°$. At angles α of 75°, 60°, and 45°, the change in mass was 0.195, 0.178, and 0.231 g, respectively.

Conclusions

The studies conducted on the influence of ultrasonic *SPD* with different inclination angles of the working tool on the surface properties of steel 45 specimens have revealed the features of this technological method.

The studies have shown that the inclination angle of the working tool has a different effect on the characteristics of the surface layer controlled in the study.

Ultrasonic *SPD* under the selected processing modes allows reducing the height roughness parameters by up to 6–7 times, the spacing parameters by up to 3 times, and also increasing the relative bearing length of the profile by up to 4 times. Moreover, the best results are achieved at an inclination angle of $\alpha = 45°$.

The maximum depth of the work-hardened layer is achieved at $\alpha = 90°$, and under the selected processing modes, it is 345 μm. As the angle α decreases, the normal component of the force of interaction between the tool and the workpiece decreases, and the work hardening decreases accordingly. The lowest wear is also observed at the greatest depth of work hardening.

Based on the conducted studies, it can be stated that the choice of the oscillating system inclination angle is made based on the requirements for the resulting surface layer. In cases where it is necessary to obtain the lowest values of the roughness parameters, it is advisable to set the inclination angle to $\alpha = 45$–60°. The greatest depth of the deformed layer and, as a consequence, greater wear resistance is achieved at $\alpha = 75°…90°$.

Since, as noted, the most significant factors are feed and clamping force, the obtained results can be used in the processing of curved surfaces of parts, in particular, those obtained by additive manufacturing technologies. In such cases, the ultrasonic equipment is installed on a machine that provides the required strategy for moving the working tool, while the most rational technological method is to regulate the oscillating system inclination angle during processing.

References

1. Radchenko V.P., Saushkin M.N., Bochkova T.I. A mathematical modeling and experimental study of forming and relaxation of the residual stresses in plane samples made of EP742 alloy after the ultrasonic hardening under the high-temperature creep conditions. *PNRPU Mechanics Bulletin*, 2016, vol. 1, pp. 93–112. DOI: 10.15593/perm.mech/2016.1.07.

2. Krylova N.A., Shuvaev V.G. Obespechenie nadezhnosti i kachestva poverkhnostei detalei ul'trazvukovym poverkhnostnym plasticheskim deformirovaniem [Ensuring the reliability and quality of surfaces of parts by ultrasonic surface plastic deformation]. *Nadezhnost' i kachestvo = Reliability and Quality*, 2018, vol. 2, pp. 205–206.

3. Abramov O.V., Prikhod'ko V.M., ed. *Moshchnyi ul'trazvuk v metallurgii i mashinostroenii* [Powerful ultrasound in metallurgy and mechanical engineering], Moscow, Yanus-K Publ., 2006. 687 p. ISBN 5-8037-0314-1.

4. Bai F., Saalbach K.-A., Wang L., Wang X., Twiefel J. Impact of time on ultrasonic cavitation peening via detection of surface plastic deformation, *Ultrasonics*, 2018, vol. 84, pp. 350–355. DOI: 10.1016/j.ultras.2017.12.001.

5. Zhang Y., Huang L., Lu F., Qu S., Ji V., Hu X., Liu H. Effects of ultrasonic surface rolling on fretting wear behaviors of a novel 25CrNi2MoV steel. *Materials Letters*, 2021, vol. 284 (2), p. 128955. DOI: 10.1016/j.matlet.2020.128955.

6. Cui Z., Mi Y., Qiu D., Dong P., Qin Z., Gong D., Li W. Microstructure and mechanical properties of additively manufactured CrMnFeCoNi high-entropy alloys after ultrasonic surface rolling process. *Journal of Alloys and Compounds*, 2021, vol. 887, pp. 161393. DOI: 10.1016/j.jallcom.2021.161393.

7. Lai F., Qu S., Lewis R., Slatter T., Fu W., Li X. The influence of ultrasonic surface rolling on the fatigue and wear properties of 23-8N engine valve steel. *International Journal of Fatigue*, 2019, vol. 125, pp. 299–313. DOI: 10.1016/j.ijfatigue.2019.04.010.

8. Rosenberg L.D., ed. *Fizika i tekhnika moshchnogo ul'trazvuka*. Kn. 3 [Physics and technology of powerful ultrasound. Vol. 3]. Moscow, Nauka Publ., 1970. 689 p.

9. Manokhin A.I., ed. *Vozdeistvie moshchnogo ul'trazvuka na mezhfaznuyu poverkhnost' metallov* [The effect of powerful ultrasound on the interphase surface of metals]. Moscow, Nauka Publ., 1986. 277 p.

10. Suslov A.G., ed. *Spravochnik tekhnologa* [Technologist's handbook]. Moscow, Innovatsionnoe mashino-stroenie Publ., 2019. 800 p. ISBN 978-5-907104-23-5.

11. Li G., Qu S.G., Pan Y.X., Li X.Q. Effects of the different frequencies and loads of ultrasonic surface rolling on surface mechanical properties and fretting wear resistance of HIP Ti–6Al–4V alloy. *Applied Surface Science*, 2016, vol. 389, pp. 324–334. DOI: 10.1016/j.apsusc.2016.07.120.

12. Li G., Qu S., Xie M.M., Li X. Effect of ultrasonic surface rolling at low temperatures on surface layer microstructure and properties of HIP Ti-6Al-4V alloy. *Surface and Coatings Technology*, 2017, vol. 316, pp. 75–84. DOI: 10.1016/j.surfcoat.2017.01.099.

13. Li G., Qu S., Xie M., Ren Z., Li X. Effect of multi-pass ultrasonic surface rolling on the mechanical and fatigue properties of HIP Ti-6Al-4V alloy. *Materials*, 2017, vol. 10, p. 133. DOI: 10.3390/ma10020133.

14. Luan X., Zhao W., Liang Z., Xiao S., Liang G., Chen Y., Zou S., Wang X. Experimental study on surface integrity of ultra-high-strength steel by ultrasonic hot rolling surface strengthening. *Surface and Coatings Technology*, 2020, vol. 392, p. 125745. DOI: 10.1016/j.surfcoat.2020.125745.

15. Zhao W., Liu D., Qin H., Zhang X., Zhang H., Zhang R., Ren Z., Ma C., Amanov A., Pyun Y.-S., Doll G.L., Dong Y., Ye C. The effect of ultrasonic nanocrystal surface modification on low temperature nitriding of ultra-high strength steel. *Surface and Coatings Technology*, 2019, vol. 375, pp. 205–214. DOI: 10.1016/j. surfcoat.2019.07.006.

16. Ting W., Dongpo W., Gang L., Baoming G., Ningxia S. Investigations on the nanocrystallization of 40Cr using ultrasonic surface rolling processing. *Applied Surface Science*, 2008, vol. 255 (5), pp. 1824–1829. DOI: 10.1016/j. apsusc.2008.06.034.

17. John M., Ralls A.M., Dooley S.C., Thazhathidathil A.K.V., Perka A.K., Kuruveri U.B., Menezes P.L. Ultrasonic surface rolling process: properties, characterization, and applications. *Applied Sciences*, 2021, vol. 11 (22), p. 10986. DOI: 10.3390/app112210986.

18. Kazantsev V.F., Kudryashov B.A., Neverov A.N., Nigmetzyanov R.I., Prikhod'ko V.M. *Primenenie ul'trazvuka pri sborochno-razborochnykh operatsiyakh* [The use of ultrasound in assembly and disassembly operations]. Moscow, Tekhpoligraftsentr Publ., 2008. 145 p. ISBN 978-5-94385-040-0.

19. Prikhod'ko V.M. *Ul'trazvukovye tekhnologii pri proizvodstve i remonte avtotraktornoi tekhniki* [Ultrasonic technologies in the production and repair of automotive equipment]. Moscow, Tekhpoligraftsentr Publ., 2000. 252 p. ISBN 5-900095-16-9.

20. Cao X.J., Pyoun Y.S., Murakami R. Fatigue properties of a S45C steel subjected to ultrasonic nanocrystal surface modification. *Applied Surface Science*, 2010, vol. 256 (21), pp. 6297–6303. DOI: 10.1016/j.apsusc. 2010.04.007.

21. Mukhanov I.I., Golubev Yu.M. Uprochnenie stal'nykh detalei sharikom, vibriruyushchim s ul'trazvukovoi chastotoi [Hardening of steel parts with a ball vibrating at ultrasonic frequency]. *Vestnik mashinostroeniya = Russian Engineering Research*, 1966, vol. 11, pp. 52–53. (In Russian).

22. Stebel'kov I.A. *Sposob poverkhnostnogo uprochneniya* [Surface hardening method]. Inventor's Certificate USSR, no. 456704, 1975.

23. Nigmetzyanov R.I., Prikhodko V.M., Sundukov S.K., Sukhov A.V., Fatyukhin D.S. Sposoby ul'trazvukovogo poverkhnostnogo plasticheskogo deformirovaniya [Methods of ultrasonic surface plastic deformation]. *Naukoemkie tekhnologii v mashinostroenii = Science Intensive Technologies in Mechanical Engineering*, 2022, vol. 7 (133), pp. 33–39. DOI: 10.30987/2223-4608-2022-1-7-33-39.

24. Jerez-Mesa R., Travieso-Rodriguez J.A., Gómez-Gras G., Llumà-Fuentes J. Development, characterization and test of an ultrasonic vibration-assisted ball burnishing tool. *Journal of Materials Processing Technology*, 2018, vol. 257, pp. 203–212. DOI: 10.1016/j.jmatprotec.2018.02.036.

25. Liu P., Yu R., Gao X., Zhang G. Influence of surface ultrasonic rolling on microstructure and corrosion property of T4003 ferritic stainless steel welded joint. *Metals*, 2020, vol. 10, p. 1081. DOI: 10.3390/met10081081.

26. Wang C., Han J., Zhao J., Song Y., Man J., Zhu H., Sun J., Fang L. Enhanced wear resistance of 316 L stainless steel with a nanostructured surface layer prepared by ultrasonic surface rolling. *Coatings*, 2019, vol. 9, p. 276. DOI: 10.3390/coatings9040276.

27. Nigmetzyanov R.I., Prikhod'ko V.M., Sundukov S.K., Sukhov A.V., Fatyukhin D.S. Optimizing the parameters of ultrasonic surface plastic deformation by a free steel indenter. *Russian Engineering Research*, 2022, vol. 42 (11), pp. 1195–1198. DOI: 10.3103/s1068798x22110181.

28. Kazantsev V.F., Luzhnov Yu.M., Nigmetzyanov R.I., Sundukov S.K., Fatyukhin D.S. Vybor i optimizatsiya rezhimov ul'trazvukovogo poverkhnostnogo deformirovaniya [Selection and optimization of ultrasonic surface deformation modes]. *Vestnik Moskovskogo avtomobil'no-dorozhnogo gosudarstvennogo tekhnicheskogo universiteta (MADI) = Bulletin of the Moscow Automobile and Road Construction State Technical University (MADI)*, 2016, vol. 4 (47), pp. 26–32.

29. Britvin L.N., Germanova V.A., Karagodin V.I., Nigmetzyanov R.I., Fatyukhin D.S. Uprochnenie poverkhnostnogo sloya detalei mashin metodami khimiko-termicheskoi obrabotki i ul'trazvukovymi tekhnologiyami [Hardening of the surface layer of machine parts using chemical-thermal treatment methods and ultrasonic technologies]. *Vestnik Moskovskogo avtomobil'no-dorozhnogo gosudarstvennogo tekhnicheskogo universiteta (MADI) = Bulletin of the Moscow Automobile and Road Construction State Technical University (MADI)*, 2017, vol. 1 (48), pp. 63–67.

30. Sundukov S.K., Nigmetzyanov R.I., Prikhodko V.M., Fatyukhin D.S. Sequential treatment of steel surfaces by nitriding and ultrasonic hardening. *Key Engineering Materials*, 2022, vol. 910, pp. 484–489. DOI: 10.4028/p-vz1gn6.

31. Chudina O.V., Prikhod'ko V.M., Simonov D.S., Bringulis P. Hybrid technology for surface hardening of structural steel. *Russian Engineering Research*, 2022, Vol. 42 (11), pp. 1192–1194. DOI: 10.3103/s1068798x22110065.

32. Chudina O., Simonov D., Simonova T., Litovchenko A. Effective combined surface hardening processes of structural steels using ultrasound. *E3S Web of Conferences*, 2023, vol. 431, p. 06024. DOI: 10.1051/e3sconf/202343106024.

33. Salmi M., Huuki J., Ituarte I.F. The ultrasonic burnishing of cobalt-chrome and stainless steel surface made by additive manufacturing. *Progress in Additive Manufacturing*, 2017, vol. 2, pp. 31–41. DOI: 10.1007/s40964-017-0017-z.

34. Ojo S.A., Manigandan K., Morscher G.N., Gyekenyesi A.L. Enhancement of the microstructure and fatigue crack growth performance of additive manufactured titanium alloy parts by laser-assisted ultrasonic vibration processing. *Journal of Materials Engineering and Performance*, 2024, vol. 33, pp. 10345–10359. DOI: 10.1007/s11665-024-09323-8.

35. Xu Q., Qiu Z., Jiang D., Cai G., Yang X., Liu J., Li G. Surface properties of additively manufactured 316L steel subjected to ultrasonic rolling. *Journal of Materials Engineering and Performance*, 2024, pp. 1–10. DOI: 10.1007/s11665-024-09173-4.

36. Walker P., Malz S., Trudel E., Nosir S., ElSayed M.S.A., Kok L. Effects of ultrasonic impact treatment on the stress-controlled fatigue performance of additively manufactured DMLS Ti-6Al-4V alloy. *Applied Sciences*, 2019, vol. 9 (22), p. 4787. DOI: 10.3390/app9224787.

37. Fatyukhin D.S., Nigmetzyanov R.I., Prikhodko V.M., Sukhov A.V., Sundukov S.K. Comprehensive estimation of changes in the microgeometry of steel 45 by ultrasonic plastic deformation with a free deforming element. *Metals*, 2023, vol. 13 (1), p. 114. DOI: 10.3390/met13010114.

38. *Universal friction machine MTU-01. TU 32.99.53-001-78940767-2018*. Operation manual. LLC Advanced Technologies Publ., 2023. 18 p. (In Russian).

Conflicts of Interest

The authors declare no conflict of interest.